J. Fluid Mech. (1981), *vol.* 113, *pp.* 387–405
Printed in Great Britain

Experimental study of double-diffusive cellular convection due to a uniform lateral heat flux

By U. NARUSAWA AND Y. SUZUKAWA
Technical Research Center, Nippon Kokan K.K., Kawasaki, Japan

(Received 25 September 1980 and in revised form 23 March 1981)

A uniform, lateral heat flux applied to a body of fluid with a vertical solute gradient, causes the horizontal growth of cellular convection. This paper deals with a series of experimental studies of the phenomenon, which yielded the following results. (1) The third non-dimensional parameter besides the Prandtl number and the diffusivity ratio, τ, in this particular double-diffusive convection was found to be $\pi_3 = -\alpha(q/k)/\beta(dS/dz)$ in which q, k, $-(dS/dz)$ are the lateral heat flux, the thermal conductivity of the fluid and the initial solute gradient respectively, and where $\alpha = -\rho^{-1}(\partial\rho/\partial T)$, and $\beta = \rho^{-1}(\partial\rho/\partial S)$, ρ being the density. The existence of a critical value of π_3 above which cellular convection occurs has been confirmed in this study. (2) When the solute used was varied (i.e. with τ different), the corresponding shift in the critical value of π_3 was also observed indicating that the critical values of π_3 are 0·13 for $CuSO_4$ ($\tau = 3{\cdot}5 \times 10^{-3}$), 0·28 for common salt ($\tau = 9 \times 10^{-3}$) and 0·76 for HCl ($\tau = 24 \times 10^{-3}$). (3) The measured vertical height of a cell, h, when normalized with respect to a characteristic length $L(=[\nu\kappa/g\alpha(q/k)]^{\frac{1}{4}}$ where ν and κ are the kinematic viscosity and the thermal diffusivity, respectively), increased steadily with π_3, and for a given value of π_3, h/L decreased with an increase in τ. (4) Studies of the shadowgraph pictures indicated that the initially developed roll cells quickly merge to form layers of outward-growing convection cells.

1. Introduction

The behaviour of a fluid in which there are gradients of two properties with different molecular diffusivities is called 'double-diffusive convection'. Although the name 'double-diffusive convection' covers a wide range of phenomena (see Turner 1979), we shall restrict ourselves here to the discussion of a body of fluid with a vertical solute gradient heated at its boundary; a situation in which layers of fluid form, separated at their top and bottom by a sharp density interface.

Turner & Stommel (1964) and Turner (1968) investigated the behaviour of a fluid with a density gradient created by salt concentration and with a uniform heat flux applied at the bottom. Turner's theoretical analysis combined with experimentation gave the growth rate of the first layer adjacent to the heated bottom as well as the criteria for the successive layer formation above the first. On the other hand, Thorpe, Hutt & Soulsby (1969) studied the layer formation (cellular convection) in a fluid with a linear salt gradient heated at its vertical side wall. They developed a stability analysis for a fluid with a vertical salt concentration gradient and a horizontal temperature gradient contained in a slot between hot and cold walls, followed by an

experiment in which fluid with a salt concentration gradient was placed in slots of 3·5 and 6·0 mm widths with the wall temperatures kept constant. Their results showed that the relationship between a thermal Rayleigh number and a solute Rayleigh number based on the slot width describes the onset of cellular convection.

Chen, Briggs & Wirtz (1971) have studied the onset of cellular convection along a heated wall when the presence of the opposite wall is not felt by the convecting fluid, i.e. the onset of cellular convection in a semi-infinite body of fluid. They showed experimentally that for an aqueous solution of salt (i.e. fixed values of the Prandtl number and the diffusivity ratio) the motion of fluid is determined by the Rayleigh number, $Ra = g\alpha\Delta T(\nu\kappa)^{-1}(-\alpha\Delta T/\beta(dS/dz))^3$ where α and β have already been defined, and g, ν, κ, ΔT, $-dS/dz$ and ρ are the gravitational acceleration, the kinematic viscosity, the thermal diffusivity, the temperature difference between the wall and the fluid, the vertical solute gradient in the fluid and the density of the fluid respectively. It should be noted that the experimental results of both Thorpe *et al.* (1969) and Chen *et al.* (1971) were obtained for a constant side-wall temperature.

Numerical analyses on the stability of a vertical solute gradient bounded by side walls of constant temperature have been made by Hart (1971), Wirtz, Briggs & Chen (1972), Hart (1973), Chen (1974) and Wirtz & Liu (1975). Also more recently, Wirtz & Reddy (1976) have investigated the heat and mass transport across a diffusive interface bounded by turbulent regions.

All of the investigations mentioned so far have been made mainly to clarify the layered structure of the fluid, both in terms of salinity and temperature, as a recently discovered characteristic of the ocean. However, double-diffusive convection does occur in other fields of engineering interest such as in large liquid storage tanks, solar ponds and solidifying metal alloys, and the purpose of this investigation is aimed at studying the following three aspects of cellular convection with a wider range of engineering applications in mind.

Uniform heat flux at the vertical wall

The investigation of cellular convection along a vertical wall has so far been limited to the case of a constant wall temperature. However, there are many situations in which heat flux rather than wall temperature is specified, and the present study is focused on the case of a uniform heat flux similar to studies done by Turner (1968) and by Huppert & Linden (1979) for the case of bottom heating.

Effect of the diffusivity ratio

The non-dimensional parameters describing double-diffusive convection invariably include the diffusivity ratio, τ, i.e. the ratio of diffusivity of the stabilizing component to that of the destabilizing component. In this study, in order to determine the effect of τ on cellular convection, three different solutes (i.e. NaCl, HCl and $CuSO_4$) were used as the stabilizing components while heat is used as the destabilizing component. Because of the large value of thermal diffusivity, κ, compared with that of mass diffusivity, κ_s, the range of τ $(=\kappa_s/\kappa)$ is limited to 0·003–0·025; however, a fairly large number of liquid substances falls into this range of τ. It should also be mentioned here that the effect of τ on the heat and mass transport across a sharp diffusive interface has been studied experimentally by Takao & Narusawa (1980) whose results indicated a marked effect of the difference in solute on heat and mass transfer.

Cell size study

Chen *et al.* (1971) showed experimentally that the vertical size of a cell, h, is roughly of the order of $-\alpha\Delta T/\beta(dS/dz)$ for the case of a constant wall temperature. A similar study will be made for the case of a uniform heat flux. When the vertical solute concentration gradient is absent, natural convection with a boundary layer along the vertical wall occurs. In order to clarify this transition of the fluid behaviour, cellular convection for a very small concentration gradient with a large heat flux will also be studied.

In §2 we discuss a dimensional analysis formulated to determine an adequate set of non-dimensional parameters, followed by a description of the experiment in §3 and a discussion of its results in §4.

2. Non-dimensional analysis

Here the non-dimensional parameters, which describe the behaviour of the fluid, will be sought by writing down the equations relevant to our dimensional analysis. Let $x = 0$ be the location of the wall with a uniform heat flux, q, and the region of $x > 0$ be a semi-infinite body of fluid with an initial solute gradient, $-dS/dz$, where the z direction is taken as positive upwards. If u and v are the velocities in the x and z directions respectively, the continuity, momentum, energy and solute equations are

$$\frac{\partial u}{\partial x}+\frac{\partial v}{\partial z} = 0, \tag{1}$$

$$\frac{D}{Dt}\left(\frac{\partial u}{\partial z}-\frac{\partial v}{\partial x}\right) = \nu\nabla^2\left(\frac{\partial u}{\partial z}-\frac{\partial v}{\partial x}\right)-g\left(\alpha\frac{\partial T}{\partial x}-\beta\frac{\partial S}{\partial x}\right), \tag{2}$$

$$\frac{DT}{Dt} = \kappa\nabla^2 T, \quad \frac{DS}{Dt} = \kappa_s\nabla^2 S, \tag{3), (4}$$

where T and S are the temperature and the solute concentration respectively. Equation (2) has been obtained by cancelling the pressure terms from the momentum equations in the x and z directions and also by noting that

$$\frac{1}{\rho_0}\frac{\partial \rho'}{\partial x} = -\alpha\frac{\partial T}{\partial x}+\beta\frac{\partial S}{\partial x},$$

where ρ_0 is the reference density and ρ' is the deviation from ρ_0.

A boundary condition relevant to our dimensional analysis is

$$q = -k\frac{\partial T}{\partial x} \quad \text{at} \quad x = 0, \tag{5}$$

where q is the heat flux at the wall and k is the thermal conductivity of the liquid. Now define the following non-dimensional quantities, $x = L\bar{x}$, $z = L\bar{z}$, $u = (\kappa/L)\bar{u}$, $v = (\kappa/L)\bar{v}$, $t = (L^2/\kappa)\bar{t}$, $S-S_R = -\bar{S}L(dS/dz)$ and $T-T_R = \bar{T}\Delta T_R$, where bars indicate non-dimensional quantities, and L, S_R, T_R and ΔT_R are the reference scales. Then (1)–(5) become

$$\frac{\partial \bar{u}}{\partial \bar{x}}+\frac{\partial \bar{v}}{\partial \bar{z}} = 0, \tag{6}$$

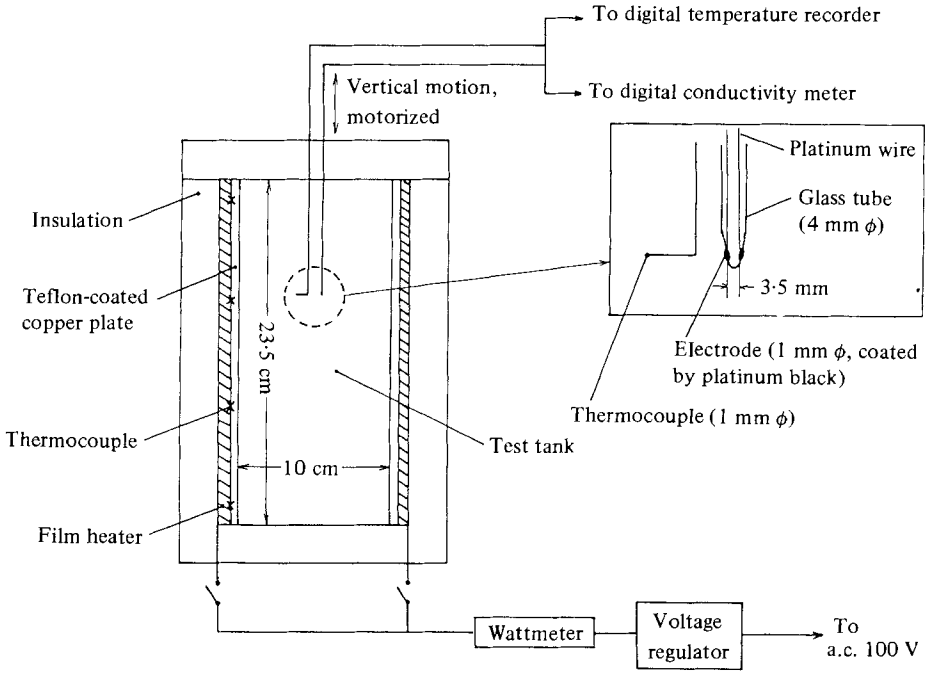

FIGURE 1. Schematic diagram of the test apparatus.

$$\frac{1}{(\nu/\kappa)}\frac{D}{D\bar{t}}\left(\frac{\partial\bar{u}}{\partial\bar{z}}-\frac{\partial\bar{v}}{\partial\bar{x}}\right)=\bar{\nabla}^2\left(\frac{\partial\bar{u}}{\partial\bar{z}}-\frac{\partial\bar{v}}{\partial\bar{x}}\right)-\frac{g\alpha\Delta T_R L^3}{\nu\kappa}\frac{\partial\bar{T}}{\partial\bar{x}}-\frac{g\beta(dS/dz)L^4}{\nu\kappa}\frac{\partial\bar{S}}{\partial\bar{x}}, \tag{7}$$

$$\frac{D\bar{T}}{D\bar{t}}=\bar{\nabla}^2\bar{T}, \quad \frac{D\bar{S}}{D\bar{t}}=\frac{\kappa_s}{\kappa}\bar{\nabla}^2\bar{S}, \tag{8), (9}$$

$$q=-k\frac{\Delta T_R}{L}\frac{\partial\bar{T}}{\partial\bar{x}} \quad \text{at} \quad \bar{x}=0. \tag{10}$$

If, in the above set of equations, ΔT_R and L are defined so that

$$\Delta T_R=\frac{q}{k}L \quad \text{and} \quad L=\left[\frac{\nu\kappa}{g\alpha(q/k)}\right]^{\frac{1}{4}},$$

we arrive at the following three non-dimensional parameters,

$$\text{Prandtl number} \quad \pi_1=\nu/\kappa=Pr,$$

$$\text{diffusivity ratio} \quad \pi_2=\kappa_s/\kappa=\tau,$$

and

$$\pi_3=-\alpha(q/k)/\beta(dS/dz).$$

Compared with the case of a constant wall temperature in which the natural length scale is $-\alpha\Delta T/\beta(dS/dz)$ (the height to which a heated fluid element would rise in the initial solute gradient), our case of a uniform heat flux does not present a natural length scale. However, in the analysis of natural convection in a rectangular cavity with its two vertical sides maintained at different temperatures, Gill (1966) showed that the quantity, $[\nu\kappa H/\alpha g\Delta T]^{\frac{1}{4}}$ (where H is the vertical length scale), is associated with the thickness of the boundary layers on the vertical walls. Our reference length

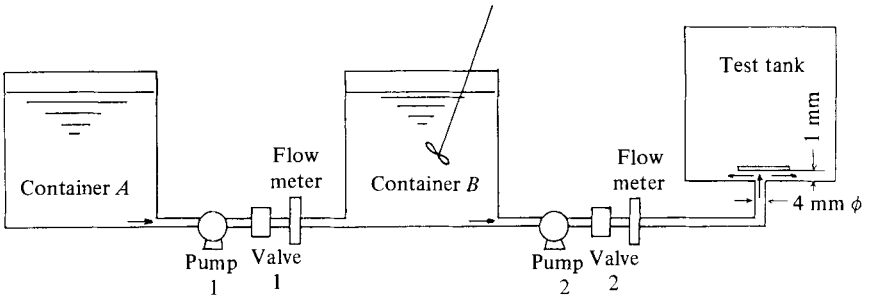

FIGURE 2. Apparatus for producing linear solute gradients in the test tank.

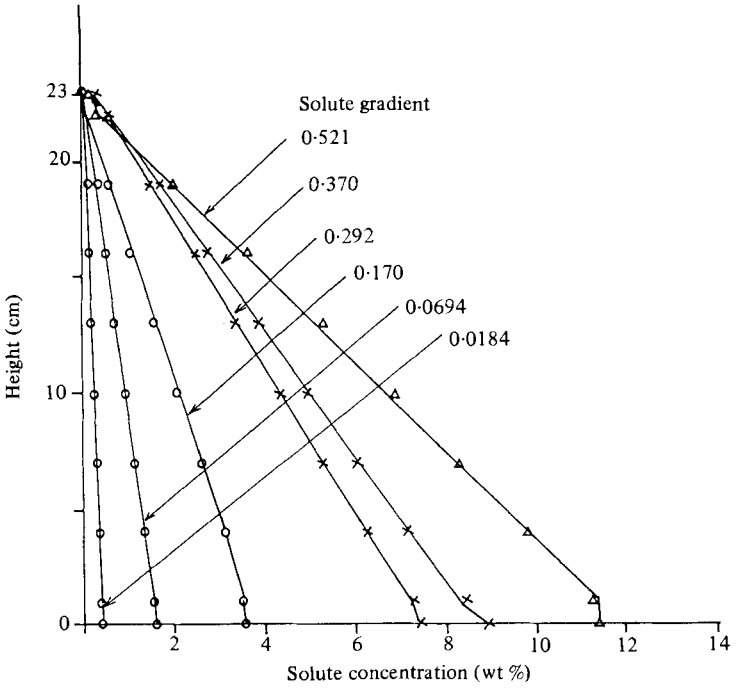

FIGURE 3. Examples of the solute gradient produced in the test tank. (Solute = common salt.)

scale, L, can also be interpreted as the horizontal length scale associated with a thermal boundary layer in the absence of the vertical solute gradient. The third parameter, π_3, can be interpreted as the ratio of the thermal Rayleigh number to the solute Rayleigh number. Based on these non-dimensional parameters, a series of experiments which will be discussed henceforth, was performed.

3. Experiment

Figure 1 is a schematic diagram of the test apparatus. The tank is 23·5 cm high by 16 cm deep by 10 cm wide, and consists of two copper (23·5 × 16 cm) and two acrylic side walls with an acrylic bottom. The acrylic plates used for both the side walls and the bottom are 1·5 cm thick, while the thickness of the copper plate is 1·0 mm. In

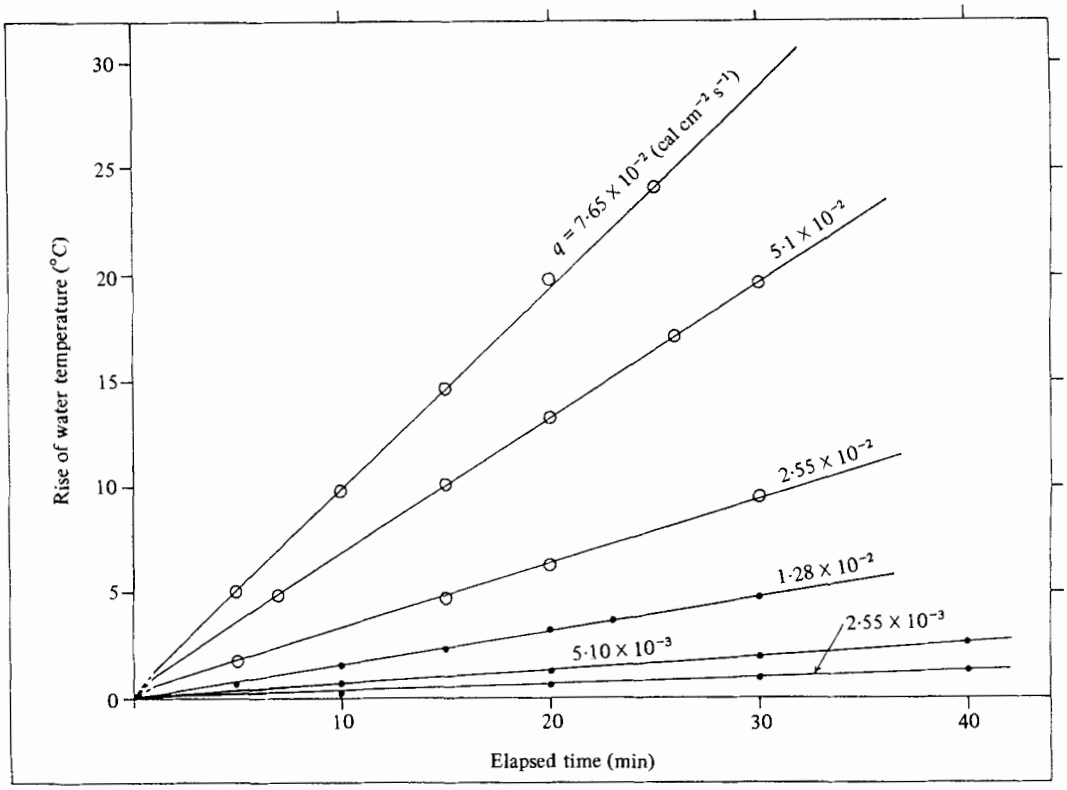

FIGURE 4. Calibration results of the heaters.

order to protect the copper plate against corrosion, the side of the plate to be in contact with the fluid is Teflon-coated (the thickness of which is less than 0·1 mm). A film type heater ('Silicone Rubber Heater' by Watlow) is attached to the back of the copper plates by a special heat-conducting cement. The heaters are connected to an a.c. 100 V supply via a digital wattmeter and a voltage regulator. The back of the copper side walls as well as the top and bottom of the tank are insulated with pads of calcium silicate, 2·5 cm thick. Four copper–constantan film thermocouples are attached to the back of the copper plates; their respective distances from the bottom of the tank being 2, 8·5, 15 and 21·5 cm.

A conductivity probe for measuring the vertical solute gradient and a copper–constantan thermocouple are mounted on a traverse mechanism. This mechanism is motorized in the vertical direction with its horizontal position adjusted manually. The quantitative relationship between the output of the conductivity gauge and the solute concentration was obtained by use of a refractometer which provided the density measurement of a sample with a known conductivity output. The refractometer has the capability of analysing a 1/1000 % difference in concentration. The gauge was used for accurate measurement of the initial solute gradients.

The linear solute gradient in the tank was formed by a modified version of the method described by Oster (1965), shown in figure 2. Container A holds an aqueous solution of common salt, $CuSO_4$ or HCl, while container B initially holds distilled water. The linear solute gradient in the test tank can be produced by keeping both

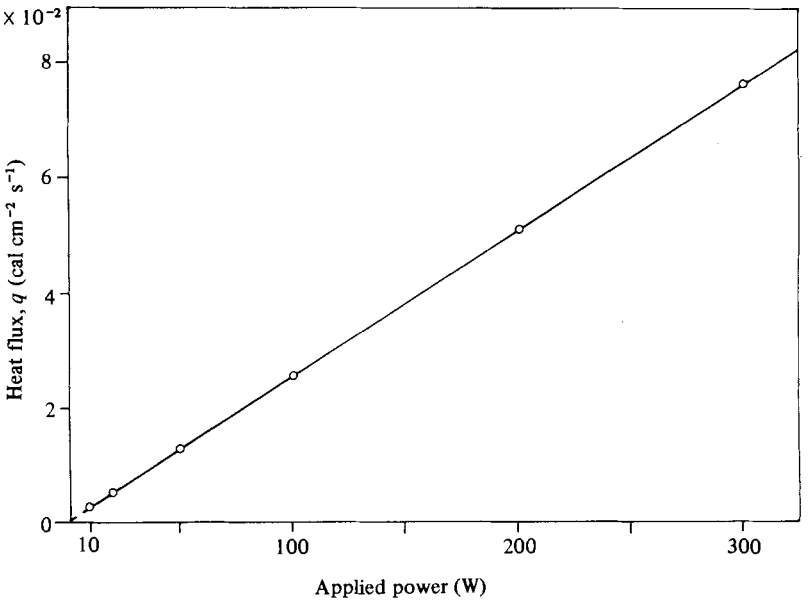

FIGURE 5. Relationship between power applied and heat flux into the fluid.

the flow rate from container A to container B and the flow rate from container B to the test tank constant (but not necessarily equal) with the manipulation of valves 1 and 2. This method enabled us to obtain an accurately linear solute gradient in the tank in a short period (~ 1 h). The linearity of the initial gradient thus produced is checked by the conductivity probe, and some of the results are shown in figure 3. It shows that the linear gradient is achieved in the range of 0·018–0·521 wt %/cm for common salt, which is a fairly wide range compared with that of the experiment by Chen *et al.* (1971), their range being 0·23–0·49 wt %/cm. Although in the high-gradient range some deviations from the linearity can be observed at the top and bottom of the tank, this does not affect our experimental results since we are interested in the fluid behaviour in the midportion of the tank. Similarly, it was confirmed that the linearity of the initial solute gradient was achieved for solutions of HCl and $CuSO_4$ in the experimental range of 0·015–0·15 wt %/cm for the former and 0·04–0·45 wt %/cm for the latter.

The relationship between the applied wattage and the heat flux into the fluid was obtained beforehand by measuring the rate of change of temperature in well-stirred water in the tank with a calibrated mercury thermometer (accuracy $\sim 0{\cdot}1$ °C). Figure 4 shows the typical calibration results. As can be seen, the initial transient period is quite short – of the order of ~ 1 min. Here, the calibration of the heater was performed for the range of 10 W to 300 W with a corresponding heat flux range of $2{\cdot}55 \times 10^{-3} - 7{\cdot}65 \times 10^{-2}$ cal cm^{-2} s^{-1}. Figure 5 shows the relationship between heat flux and applied power, which is a straight line starting at the origin. Therefore, heat flux for any applied power can be estimated from this figure. The range of heat flux used in this investigation is $0{\cdot}255 \times 10^{-3} - 0{\cdot}765 \times 10^{-1}$ cal cm^{-2} s^{-1}, i.e. a change in magnitude of 1–300.

For flow visualization we have used the shadowgraph technique because of its simplicity and capability of offering a wide view of fluid motion in the tank.

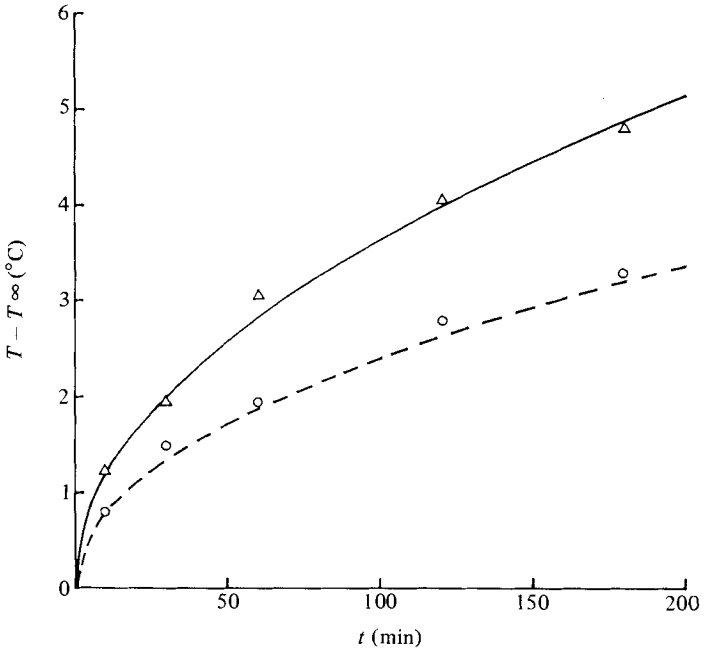

FIGURE 6. Temperature variation at the heated wall. (Solute = common salt.) △, measurement; ——, theory for $q = 1{\cdot}53 \times 10^{-3}$ cal cm^{-2} s^{-1}, $-dS/dz = 0{\cdot}179$ wt %/cm, $\pi_3 = 0{\cdot}19$. ○, measurement; - - - - -, theory for $q = 1{\cdot}02 \times 10^{-3}$ cal cm^{-2} s^{-1}, $-dS/dz = 0{\cdot}055$ wt %/cm, $\pi_3 = 0{\cdot}24$.

A typical test run began with the formation and measurement of an initial linear solute gradient with a depth of 23 cm. At this point the heaters on both copper plates were switched on and maintained at a preset value. [For some high heat flux tests, run specifically for determining the critical value of π_3, only one of the two heating surfaces was energized to check that the critical value of π_3 was not dependent on the number of heating surfaces. On the other hand, for those runs in which the measurement of the vertical height of a cell was the main purpose (i.e. for those runs in which the value of π_3 was well over critical ($\pi_3 > \sim 1{\cdot}0$)), both walls were heated to increase the number of cells to be measured, thus improving the accuracy of the data.] By adjusting the voltage regulator manually, fluctuation of the heat flux was limited to within $\pm 2\,\%$ of the average. A constant heat flux was continuously supplied until either the temperature at the vertical centre-line of the tank started to rise (this point will be further discussed in the next section) or cellular convection which developed on the two heated surfaces reached the centre of the tank. A still camera with an automatic shutter mechanism was used to provide shadowgraph pictures from which we were later able to determine both cell size and the criteria for the onset of cellular convection. All the required thermo-fluid properties were obtained from the International Critical Table (McGraw-Hill).

Before we proceed to a discussion of experimental results, the results of our preliminary investigation of applied heat flux and temperature variations on the wall as well as in the fluid will be described. In order to confirm the uniformity of temperature distribution along the heated wall as well as that of heat flux into the fluid, two test runs using common salt as a solute were performed, in which the temperature

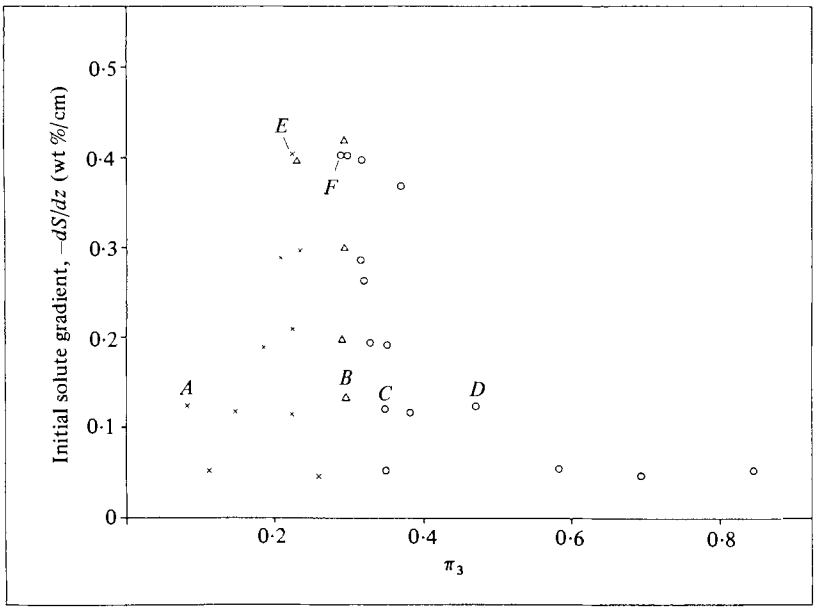

FIGURE 7. Experimental results: π_3 *vs.* initial solute gradient for common salt. ×, no occurrence of cellular convection; △, partial occurrence of cellular convection; ○, occurrence of cellular convection.

of the heated wall was monitored for a period of ~3 h. The heat flux in those tests was low enough to ensure that heat was transferred mainly by conduction. As for the uniformity of temperature along the heated wall, it was found through these tests that the deviations of temperature from the average, measured at four locations on the wall, were less than 0·2 °C. (See figure 1 for the thermocouple locations.) Figure 6 shows the measured change of temperature with time on the wall. The solution for the unsteady, one-dimensional heat conduction into a semi-infinite space is

$$T(x)-T_\infty = \frac{q\kappa^{\frac{1}{2}}}{k}\left\{2\left(\frac{t}{\pi}\right)^{\frac{1}{2}}\exp\left(-\frac{x^2}{4t\kappa}\right)-\frac{x}{\kappa^{\frac{1}{2}}}\operatorname{erfc}\left(\frac{x}{2(\kappa t)^{\frac{1}{2}}}\right)\right\}, \tag{11}$$

where x, t, T_∞ and q are the distance from the heated wall, the elapsed time, the initial temperature of the medium and the applied heat flux respectively. The wall temperature variations computed from (11) are also plotted in figure 6. From this figure, we have concluded that the condition of uniform heat flux at the wall was well-satisfied.

4. Results and discussion

Chen *et al.* (1971) observed the following from their experimental investigation: (*a*) For their Rayleigh number, Ra, below 15,000 ± 2,500, cellular convection does not occur and heat is transferred mainly by conduction in the horizontal direction, while (*b*) for $Ra > 15{,}000 \pm 2{,}500$, convection cells occur along the entire length of the heated wall. For our case of a uniform heat flux, the non-dimensional parameter corresponding to Ra is $\pi_3 = -\alpha(q/k)/\beta(dS/dz)$. Figure 7 depicts our results using common salt as a solute with cell formation indicated for various values of π_3. In this

Point	$-dS/dz$ (wt %/cm)	q (cal cm^{-2} s^{-1})	π_3	T_∞ (°C)	α (°C^{-1})	β (wt %$^{-1}$)	k (cal cm^{-1} s^{-1} °C^{-1})
A	0·129	$0{\cdot}51 \times 10^{-3}$	0·08	17·0	$0{\cdot}205 \times 10^{-3}$	$0{\cdot}713 \times 10^{-2}$	$1{\cdot}39 \times 10^{-3}$
B	0·135	$2{\cdot}04 \times 10^{-3}$	0·29	15·0	$0{\cdot}185 \times 10^{-3}$	$0{\cdot}717 \times 10^{-2}$	$1{\cdot}38 \times 10^{-3}$
C	0·121	$1{\cdot}79 \times 10^{-3}$	0·34	20·3	$0{\cdot}237 \times 10^{-3}$	$0{\cdot}707 \times 10^{-2}$	$1{\cdot}40 \times 10^{-3}$
D	0·124	$2{\cdot}30 \times 10^{-3}$	0·47	21·7	$0{\cdot}250 \times 10^{-3}$	$0{\cdot}705 \times 10^{-2}$	$1{\cdot}40 \times 10^{-3}$
E	0·401	$3{\cdot}06 \times 10^{-3}$	0·22	19·2	$0{\cdot}283 \times 10^{-3}$	$0{\cdot}702 \times 10^{-2}$	$1{\cdot}38 \times 10^{-3}$
F	0·418	$3{\cdot}70 \times 10^{-3}$	0·28	22·4	$0{\cdot}306 \times 10^{-3}$	$0{\cdot}698 \times 10^{-2}$	$1{\cdot}39 \times 10^{-3}$

TABLE 1. Some data points for the determination of the critical value of π_3 for an aqueous solution of common salt (see figure 7). T_∞ refers to the initial temperature of the fluid.

figure, × indicates that cellular convection did not occur, △ indicates a partial development of cellular convection and ○ indicates the occurrence of cellular convection along the entire wall. For runs with the initial solute gradient, $-dS/dz$, less than 0·25 wt %/cm two plates were energized, whereas for runs in which $(-dS/dz)$ is over 0·25 wt %/cm only one plate was heated. For those data points in figure 7 in which two walls were energized, the range of heat flux was $0{\cdot}5 \times 10^{-3} - 2{\cdot}5 \times 10^{-3}$ cal cm^{-2} s^{-1}, while for those in which only one wall was energized, the range was $2{\cdot}0 \times 10^{-3} - 4{\cdot}5 \times 10^{-3}$ cal cm^{-2} s^{-1}. According to (11) the elapsed time at which the temperature at the centre of the tank ($x = 5$ cm) would rise by 0·2 °C (= estimated accuracy of thermocouples) would be 120 min for $q = 0{\cdot}5 \times 10^{-3}$ cal cm^{-2} s^{-1}, and 60 min for $q = 2{\cdot}5 \times 10^{-3}$ cal cm^{-2} s^{-1}, whereas the elapsed time at which the temperature at the opposite end of the tank would rise by 0·2 °C would be 200 min for $q = 2{\cdot}0 \times 10^{-3}$ cal cm^{-2} s^{-1} and 140 min for $q = 4{\cdot}5 \times 10^{-3}$ cal cm^{-2} s^{-1}. Although a systematic monitoring of temperature inside the fluid was not done for each run, the test runs in which cells did not form were continued until the temperature rise at the centre of the tank was ~2–3 °C.

Now, observation of cell formation will be described below for the data points *A*, *B*, *C* and *D* (data for two-wall heating) and *E* and *F* (data for one-wall heating) in figure 7. (See table 1 for the listing of data.) At $\pi_3 = 0{\cdot}08$ (point *A* in figure 7, with $q = 0{\cdot}5 \times 10^{-3}$ cal cm^{-2} s^{-1}), two cells, one at the top and the other at the bottom of the tank, formed at the elapsed time of $t = 60$ min, but the rest of the side wall remained free of cells even after a constant heat flux was maintained for five hours. The appearance of the cells at the top and the bottom of the tank is believed to be due to the irregular solute gradient and the presence of the boundary. Test runs with respective π_3 values of 0·15 and 0·22 (two data points between point *A* and point *B* in figure 7) resulted in the same phenomenon. When the value of π_3 is further increased to 0·29 (point *B* in figure 7, $q = 2 \times 10^{-3}$ cal cm^{-2} s^{-1}), cells appeared at $t = 180$ min in the middle of the side wall, increasing their number to occupy about one third of the entire height. This state remained until the end of the run ($t = 250$ min). At $\pi_3 = 0{\cdot}34$ (point *C* in figure 7, $q = 1{\cdot}8 \times 10^{-3}$ cal cm^{-2} s^{-1}), convection cells appeared in the middle of the tank at $t = 60$ min and the entire side wall was covered with cells by $t = 190$ min. As the value of π_3 is increased to 0·47 (point *D* in figure 7, $q = 2{\cdot}3 \times 10^{-3}$ cal cm^{-2} s^{-1}), cells started to form in the midsection at $t = 60$ min, completing the cell formation along the entire wall by $t = 120$ min. For high solute gradient runs with only one wall heated, the cells did not form even after an elapsed time of 300 min for point *E* ($q = 3{\cdot}1 \times 10^{-3}$ cal cm^{-2} s^{-1}), while cell formation was initiated at

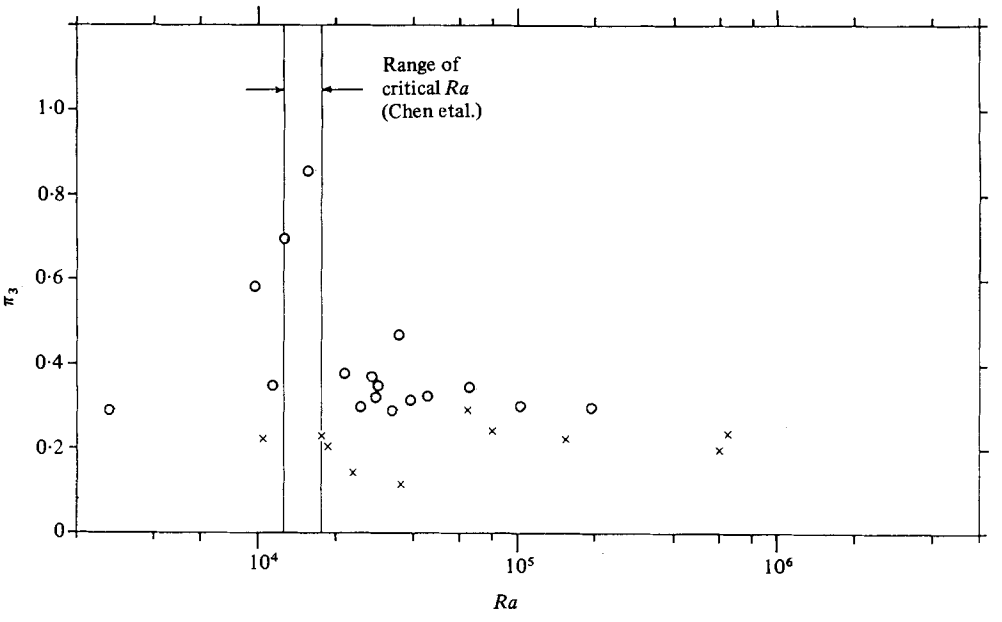

FIGURE 8. Experimental results: π_3 *vs.* Ra for common salt, where $Ra = g\alpha\Delta T/\nu\kappa(-\alpha\Delta T/\beta(dS/dz))^3$.

$t = 40$ min and was completed at $t = 100$ min for point F ($q = 3{\cdot}7 \times 10^{-3}$ cal cm^{-2} s^{-1}).

Since for our case of a uniform heat flux the wall temperature increases indefinitely with time, the question arises as to whether cellular convection always appears for the case of a lateral heat flux with the wall temperature eventually attaining a value for which the Rayleigh number defined by Chen *et al.* is above the critical (assuming the criterion based on the wall temperature is applicable). In order to clarify this question, data for common salt is replotted in figure 8 as π_3 *vs.* Ra. Ra here is obtained by estimating the wall temperature from the recorded temperature history and the still photographs of the cell formation. For the runs in which cellular convection did not occur, the wall temperature at the end of each run was used to compute Ra; while for the runs in which cellular convection did occur, the temperature at which the cells started to form was used. Figure 8 indicates that the fluid motion in the case of a uniform heat flux is entirely different from that in the case of a constant wall temperature analysed previously by many investigators, since for most of our data the Rayleigh number is above the range of the critical values of $15{,}000 \pm 2{,}500$. This conclusion is appropriate if the stability condition derived by Hart (1971) and Chen (1974) is considered, since the development of the temperature and concentration gradients in a uniform heat flux will be quite different from that in a constant wall temperature case. (The analyses of both Hart and Chen showed that the horizontal gradients of temperature and solute concentration are nearly the same in a region where instability sets in.)

Based on the above discussion, the critical value of π_3 is defined as the value above which cellular convection covers the entire vertical side wall. The validity of this definition is clearly justified within the range of this experiment by the data shown in figure 7.

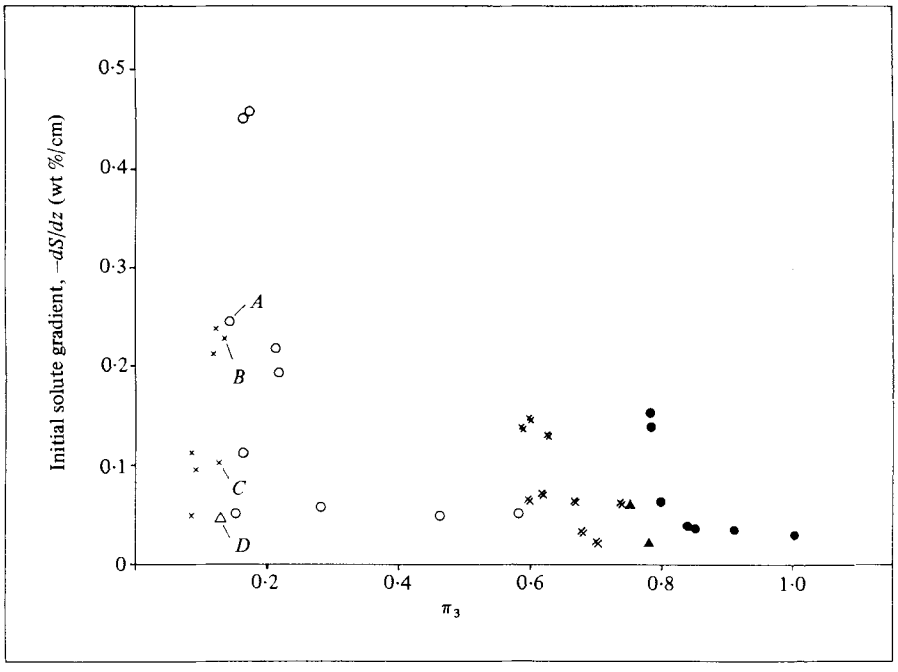

FIGURE 9. Experimental results: π_3 *vs.* initial solute gradients for $CuSO_4$ and HCl. (×, △, ○ for CuSO and ※, ▲, ● for HCl.)

Point	$-dS/dz$ (wt %/cm)	q (cal cm^{-2} s^{-1})	π_3	Comment
A	0·250	$2{\cdot}04 \times 10^{-3}$	0·14	Cell formation between t = 140 min and 240 min
B	0·247	$1{\cdot}53 \times 10^{-3}$	0·12	No cell formation after t = 240 min
C	0·105	$0{\cdot}77 \times 10^{-3}$	0·12	No cell formation after t = 300 min
D	0·049	$0{\cdot}38 \times 10^{-3}$	0·13	Partial development of cells after t = 300 min

TABLE 2. Some data points for the determination of the critical value of π_3 for an aqueous solution of $CuSO_4$ (see figure 9).

Figure 9 shows plotted data obtained using $CuSO_4$ and HCl as solutes. The data with an initial solute gradient larger than 0·2 wt %/cm in this figure was also taken with one-wall heating. For both solutes the results again indicate the existence of a critical value of π_3, above which cellular convection occurs, although the critical value itself depends on the solute used; a point that will be discussed in detail later. The experimental range for the HCl case is rather limited because of the highly corrosive nature of the solution and the risk of damage to our test equipment if used in high concentration in the middle of our investigation. From the results shown in both figures 7 and 9, it is reasonable to conclude that the non-dimensional parameter, π_3, is a correct choice for the determination of the critical condition at which cellular convection starts. It should also be noted that the zone of transition from the region of dominant conduction (i.e. no occurrence of cellular convection) into that of cellular convection is quite narrow; for instance, for the case of common salt (figure 7) the transition zone is limited to a value of π_3 between 0·26 and 0·30. In addition, the runs

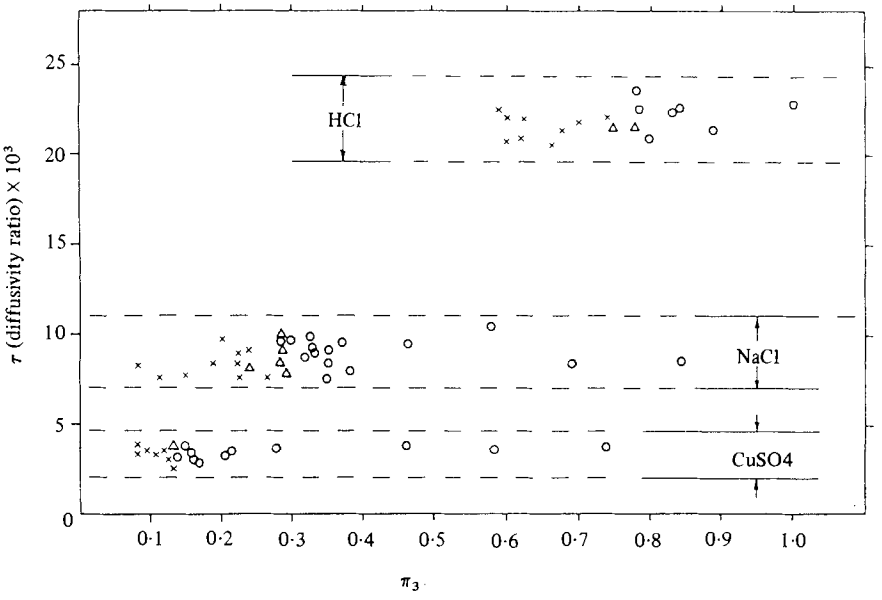

FIGURE 10. Experimental results: π_3 *vs.* the diffusivity ratio, τ.

with $CuSO_4$ as a solute yielded only one data point for a partial development of cells along the wall and the transition zone is not as clearly defined as those for NaCl and HCl. (See table 2 for the listing of representative data of $CuSO_4$ runs. They are also marked A, B, C and D in figure 9.)

The diffusivity ratio or in this case, the inverse of the Lewis number, can be interpreted as the ratio of the diffusivity of the stabilizing component to that of the destabilizing component. When the value of τ increases, one can expect the region of a stable diffusion-oriented mechanism to be sustained longer; i.e. the critical value of π_3 will increase. The effect of τ on the critical value has already been proved experimentally in a somewhat different context by Takao & Narusawa (1980) who investigated the effect of τ on the heat and mass transfer across a sharp density interface, originally studied by Turner (1965) for common salt. Their results, using $CuSO_4$, common salt and HCl as solutes, showed that the critical value of the stability parameter, R_s, increases with a decrease in the value of τ. Here, R_s is defined as $\beta\Delta S/\alpha\Delta T$ where ΔS and ΔT are solute concentration difference and temperature difference across the interface, respectively. Below this critical value of R_s, the constancy of the buoyancy flux ratio fails to hold due to turbulent motion at the breaking interface.

In this investigation a similar effect is confirmed and shown in figure 10, in which the data in figures 7 and 9 are replotted as π_3 *vs.* τ. Although the value of the diffusivity ratio for a given solute fluctuates slightly owing to changes in the solute concentration and the temperature of the solution in each run, the average values of the diffusivity ratio, τ, in this investigation are $3{\cdot}5 \times 10^{-3}$ ($CuSO_4$), 9×10^{-3} (common salt) and 24×10^{-3} (HCl) for each solute. The critical value of π_3 increases roughly linearly with τ, and from figure 10 we have concluded that the critical values of π_3 for the three solutions are 0·13 for $CuSO_4$, 0·28 for common salt and 0·76 for HCl. A possible explanation of the effect of τ on the critical value of π_3 is as follows: It is known from

No.	$q \times 10^3$ (cal cm^{-2} s^{-1})	$-dS/dz$ (wt %/cm)	T_∞ (°C)	$\alpha \times 10^3$ (°C^{-1})	$\beta \times 10^2$ (wt %$^{-1}$)	$k \times 10^2$ (cal cm^{-1} s^{-1} °C^{-1})	$\nu \times 10$ (cm^2 s^{-1})	$\kappa \times 10^2$ (cm^2 s^{-1})	$\tau \times 10^2$	π_3	h (cm)	$L \times 10$ (cm)	h/L	Solute
1	1·53	0·179	17·5	0·221	0·711	0·139	0·118	0·141	0·840	0·19	—	0·914	—	NaCl
2	2·55	0·320	20·1	0·265	0·704	0·139	0·111	0·143	0·906	0·22	—	0·758	—	
3	2·14	0·200	21·3	0·261	0·704	0·140	0·106	0·143	0·935	0·28	—	0·788	—	
4	3·82	0·422	22·7	0·309	0·697	0·140	0·104	0·144	0·995	0·29	0·59	0·651	9·03	
5	2·04	0·058	15·0	0·168	0·719	0·138	0·126	0·139	0·819	0·60	1·08	0·920	11·77	
6	11·10	0·141	21·7	0·252	0·705	0·140	0·104	0·142	0·944	2·00	1·01	0·525	19·20	
7	25·50	0·132	23·5	0·265	0·702	0·141	0·099	0·143	1·000	5·15	1·36	0·416	32·78	
8	20·40	0·051	22·6	0·243	0·705	0·141	0·101	0·142	1·020	9·81	3·15	0·452	69·74	
9	38·20	0·049	23·7	0·252	0·704	0·142	0·097	0·142	1·060	19·98	6·80	0·379	179·28	
10	0·51	0·098	25·5	0·269	1·060	0·142	0·095	0·142	0·365	0·09	—	1·090	—	$CuSO_4$
11	0·77	0·105	23·6	0·253	1·060	0·141	0·102	0·142	0·351	0·12	—	1·020	—	
12	1·53	0·247	24·5	0·273	1·040	0·141	0·105	0·142	0·328	0·12	—	0·845	—	
13	2·55	0·226	23·8	0·263	1·040	0·141	0·107	0·141	0·330	0·20	0·61	0·752	8·06	
14	2·55	0·052	21·9	0·232	1·070	0·141	0·105	0·141	0·373	0·75	1·15	0·775	14·89	
15	43·30	0·148	22·1	0·243	1·060	0·141	0·108	0·141	0·336	4·77	2·06	0·380	54·14	
16	61·20	0·139	24·8	0·266	1·060	0·142	0·099	0·142	0·346	7·84	2·71	0·334	80·95	
17	61·20	0·061	24·2	0·254	1·070	0·142	0·098	0·142	0·383	16·77	11·50	0·337	341·12	
18	2·24	0·143	23·2	0·256	0·488	0·139	0·100	0·142	2·220	0·59	—	0·770	—	HCl
19	1·33	0·069	24·2	0·256	0·489	0·141	0·096	0·142	2·170	0·72	—	0·872	—	
20	1·38	0·069	23·2	0·248	0·490	0·140	0·099	0·142	2·120	0·72	—	0·878	—	
21	0·77	0·031	26·8	0·275	0·488	0·142	0·087	0·143	2·280	0·97	1·09	0·964	11·31	
22	5·10	0·063	28·7	0·294	0·486	0·144	0·081	0·144	2·420	3·42	1·32	0·581	22·73	
23	2·55	0·015	21·8	0·227	0·497	0·141	0·104	0·141	1·970	5·43	2·24	0·775	28·90	
24	33·70	0·133	24·0	0·259	0·488	0·140	0·097	0·142	2·240	9·69	2·19	0·387	56·57	
25	10·20	0·017	26·5	0·272	0·488	0·143	0·088	0·143	2·240	23·47	7·00	0·507	138·01	

TABLE 3. Representative data points of experimental results.

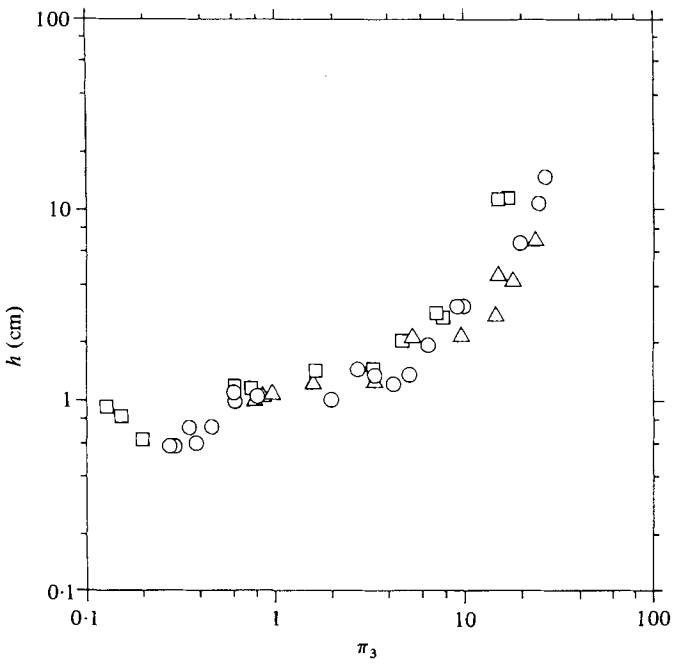

FIGURE 11. Experimental results: h (measured height of a cell) *vs.* π_3; △: HCl; ○: common salt; □: $CuSO_4$.

the analyses by Hart (1971) and by Chen (1974) that instability is initiated in a region where the horizontal gradients of temperature and salinity are nearly the same. When a lateral heat flux is applied, a horizontal temperature gradient develops in the interior of the fluid; the temperature gradient, in turn, creating a horizontal solute gradient. As the fluid element near the heated wall is lifted upward owing to the rise in temperature, the solute concentration of the fluid element decreases because of diffusion. The degree of this decrease in solute concentration depends on the value of τ; i.e. the smaller the mass diffusivity, the smaller the change in solute concentration of the fluid element. Therefore, for a given value of π_3 and κ, the horizontal solute gradient increases as κ_s (i.e. τ) decreases, thus lowering the threshold value of π_3 for the onset of diffusive instability. A similar argument holds if the decrease in τ is caused by an increase in κ.

The height of the cells was measured from the shadowgraph pictures. For small cells the size was obtained by counting the number of cells present in a known vertical distance, while for cells whose sizes were ~ 1 cm or larger, the size of each cell was directly measured and averaged. Since pictures were taken sequentially with respect to time, it was made certain that the shadowgraph pictures from which the cell sizes were measured, were taken well before the vertical heat and mass transfer across cell boundaries caused merging among cells, but after initial smaller roll cells completed merging to form a layer of outer-growing cells. Table 3 lists some representative data points. The measured size, h, is also plotted against π_3 in figure 11, showing the increase of h with π_3. Figure 12 shows the relationship between the measured cell size, h, normalized with respect to the characteristic length, L, and the non-dimensional parameter, π_3. $(h/L)^4$ can be interpreted as a Rayleigh number based on a vertical

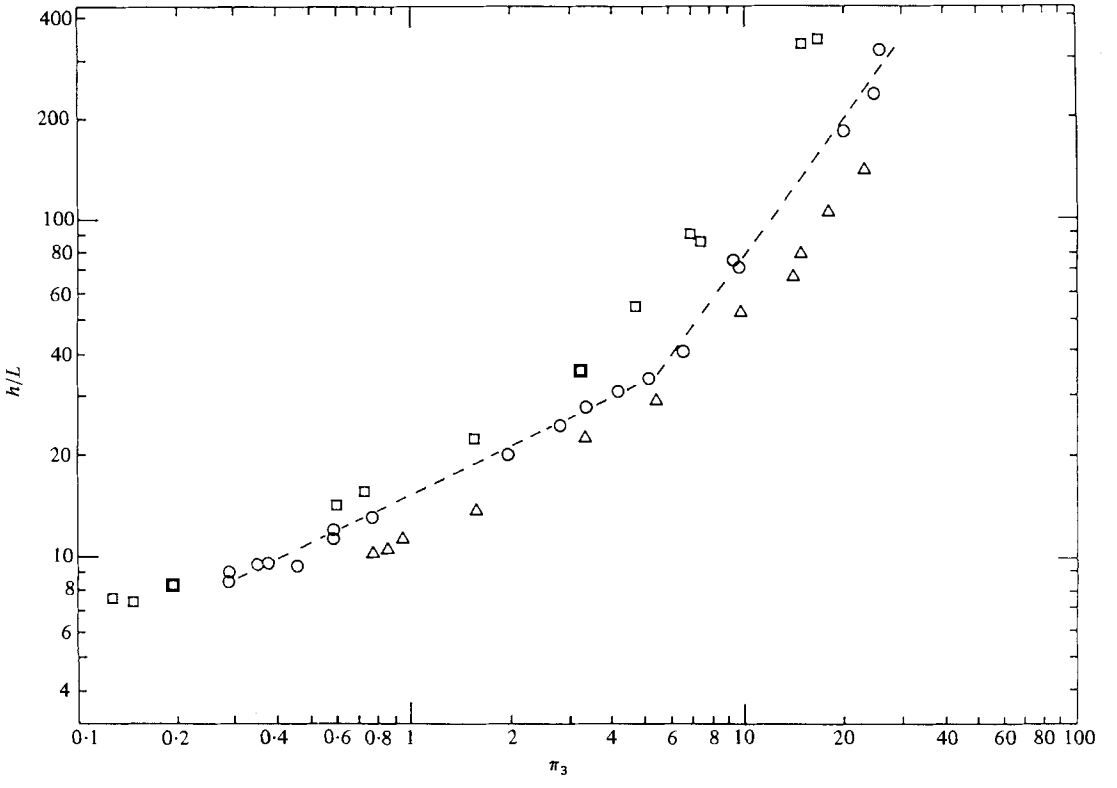

FIGURE 12. Experimental results: h/L *vs.* π_3; △: HCl; ○: common salt; □: $CuSO_4$.

temperature gradient of (q/k) and a length, h. The non-dimensional cell size, h/L, increases steadily with π_3, and the size of a cell for the case of a lower diffusivity ratio is consistently larger than that for the case of a higher diffusivity ratio for a given value of π_3. The slope of $\log(h/L)$ *vs.* $\log \pi_3$, estimated from figure 12 is approximately $\sim 0{\cdot}48$ for the range of π_3 below 3 (for $CuSO_4$), -8 (for HCl) and $\sim 1{\cdot}36$ at higher values of π_3.

When the value of π_3 exceeded ~ 30, the application of a lateral heat flux resulted either in the formation of two layers with an interface at half a fluid depth, or in the complete mixing of fluid by natural convection along the vertical wall. In our experiment, the question of whether, above a certain value of π_3 (> 30), the complete overturning of fluid would always take place was not answered because of the limitation in the available tank depth; however, our results confirm that cellular convection persists for a value of π_3 much larger than its critical value, and that if a lateral heat flux were applied to a body of fluid with an initial solute gradient and with a normalized depth smaller than h/L for a given value of π_3, it would completely overturn.

Figures 13 and 14 are two sets of sequential shadowgraph pictures illustrating the growth of cellular convection (t indicates the time elapsed after the heater is switched on). In figure 13 small roll cells start to form at $t = 3$ min 46 s, and cover the entire wall by $t = 4$ min 31 s. These roll cells will soon thereafter merge to become layers of outer-growing cells (figure 13*d*, *e*). Figure 14 shows a similar process with a larger value of π_3. It should be noted that the final size of a growing cell in this picture is

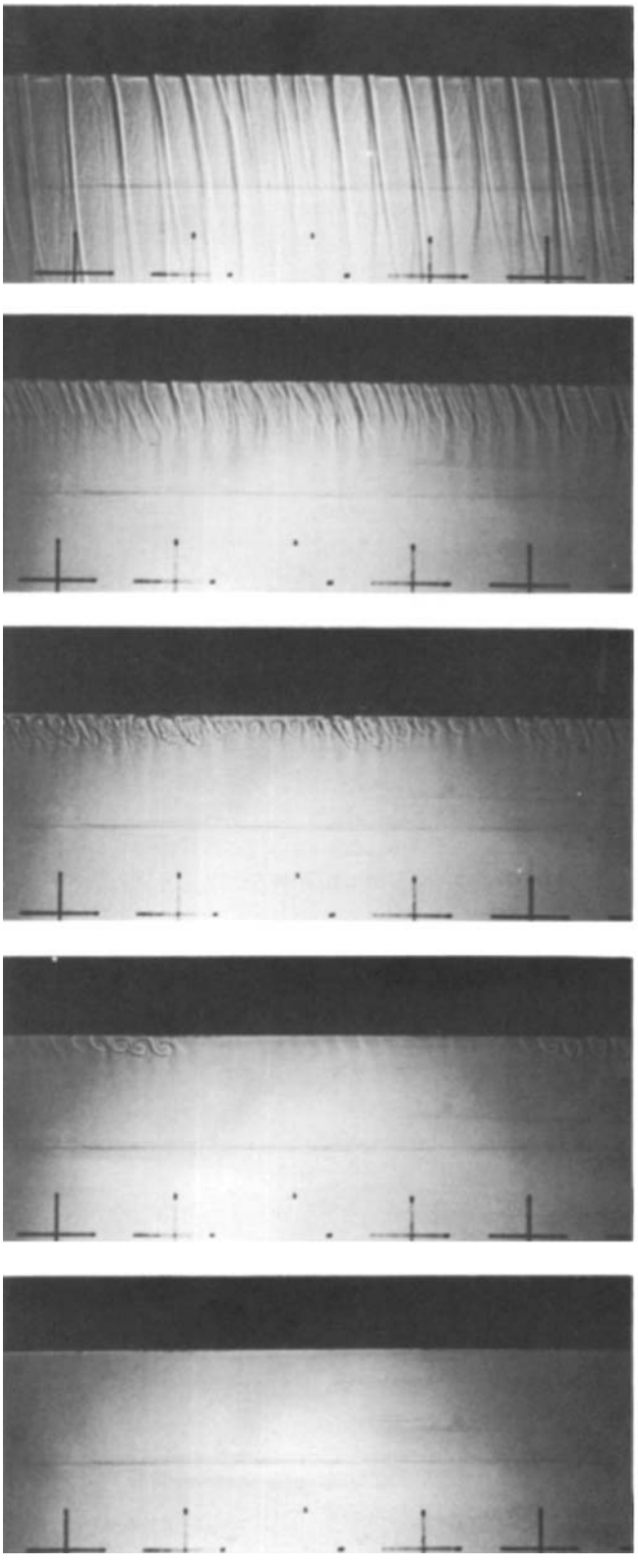

FIGURE 13. Shadowgraph pictures of cell growth. (*a*) $t = 1$ min; (*b*) $t = 3$ min 46 s; (*c*) $t = 4$ min 31 s; (*d*) $t = 6$ min 30 s; (*e*) $t = 18$ min. Solute common salt, $q = 0{\cdot}011$ cal cm^{-2} s^{-1}. $-dS/dz = 0{\cdot}141$ wt %/cm, $\pi_3 = 2{\cdot}00$, $h = \sim 1{\cdot}0$ cm.

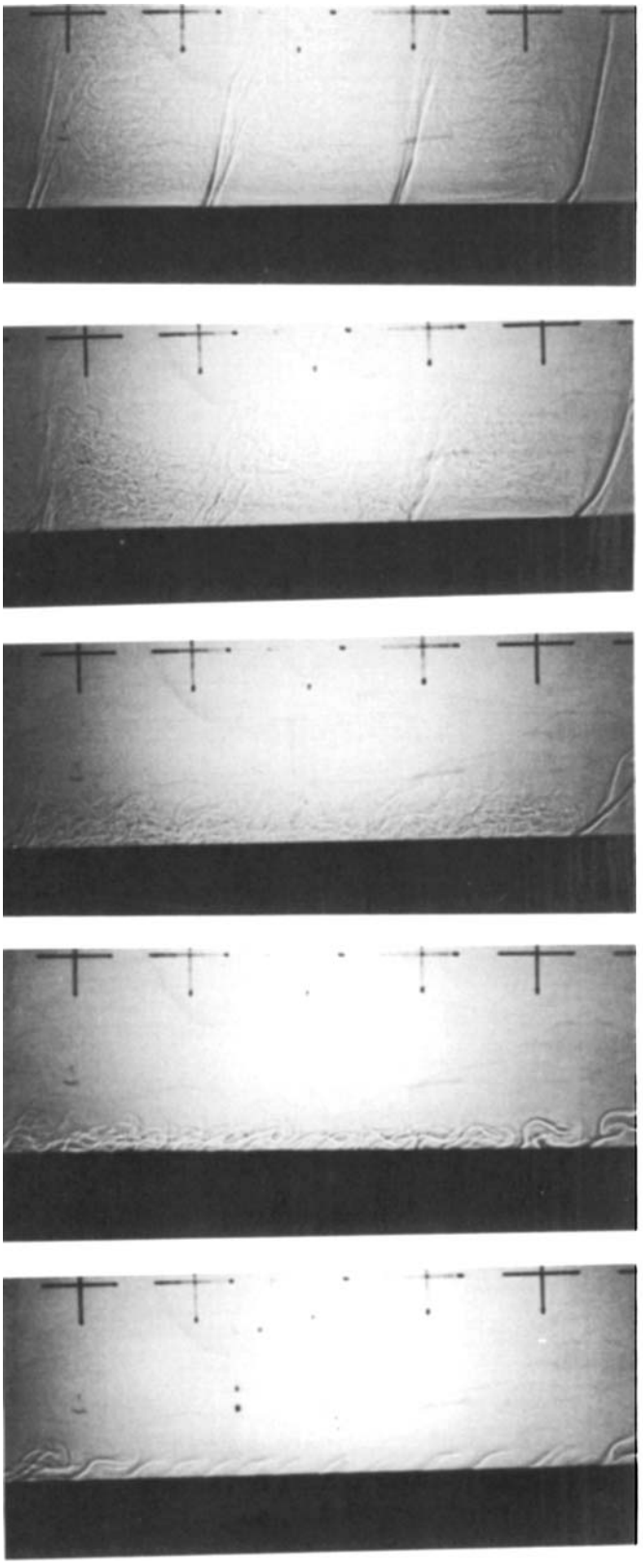

FIGURE 14. Shadowgraph pictures of cell growth. (*a*) $t = 2$ min 22 s; (*b*) $t = 2$ min 40 s; (*c*) $t = 4$ min; (*d*) $t = 7$ min; (*e*) $t = 14$ min. Solute HCl, $q = 0{\cdot}012$ cal cm^{-2} s^{-1}, $-dS/dz = 0{\cdot}028$ wt %/cm, $\pi_s = 15{\cdot}0$, $h = \sim 4{\cdot}6$ cm.

considerably larger than that of the initially-developed cells. Those growing cells, once established, exhibited a tendency to maintain a constant size, and for the merging of those cells to occur due to the vertical transport of heat and mass, it takes a time much longer than that required for the initial merging of small incipient cells, as has already been described by Chen *et al.* (1971).

REFERENCES

CHEN, C. F. 1974 Onset of cellular convection in a salinity gradient due to a lateral temperature gradient. *J. Fluid Mech.* **63**, 563–576.

CHEN, C. F., BRIGGS, D. G. & WIRTZ, R. A. 1971 Stability of thermal convection in a salinity gradient due to lateral heating. *Int. J. Heat Mass Transfer* **14**, 57–66.

GILL, A. E. 1966 The boundary-layer regime for convection in a rectangular cavity. *J. Fluid Mech.* **26**, 515–536.

HART, J. E. 1971 On sideways diffusive instability. *J. Fluid Mech.* **49**, 279–288.

HART, J. E. 1973 Finite amplitude sideways diffusive convection. *J. Fluid Mech.* **59**, 47–64.

HUPPERT, H. E. & LINDEN, P. F. 1979 On heating a stable salinity gradient from below. *J. Fluid Mech.* **95**, 431–464.

OSTER, G. 1965 Density gradients. *Scientific American* **212**, 70–76.

TAKAO, S. & NARUSAWA, U. 1980 An experimental study of heat and mass transfer across a diffusive interface. *Int. J. Heat Mass Transfer* **23**, 1283–1285.

THORPE, S. A., HUTT, P. K. & SOULSBY, R. 1969 The effect of horizontal gradients on thermohaline convection. *J. Fluid Mech.* **38**, 375–400.

TURNER, J. S. 1965 The coupled turbulent transports of salt and heat across a sharp density interface. *Int. J. Heat Mass Transfer* **8**, 759–767.

TURNER, J. S. 1968 The behaviour of a stable salinity gradient heated from below. *J. Fluid Mech.* **33**, 183–200.

TURNER, J. S. 1979 Buoyancy Effects in Fluids. Cambridge University Press.

TURNER, J. S. & STOMMEL, H. 1964 A new case of convection in the presence of combined vertical salinity and temperature gradients. *Proc. U.S. Nat. Acad. Sci.* **52**, 49–53.

WIRTZ, R. A., BRIGGS, D. G. & CHEN, C. F. 1972 Physical and numerical experiments on layered convection in a density-stratified fluid. *Geophys. Fluid Dyn.* **3**, 265–288.

WIRTZ, R. A. & LIU, L. H. 1975 Numerical experiments on the onset of layered convection in a narrow slot containing a stably stratified fluid. *Int. J. Heat Mass Transfer* **18**, 1299–1305.

WIRTZ, R. A. & REDDY, C. S. 1976 Heat and mass transport across a diffusive interface bounded by turbulent convecting regions. *Int. J. Heat Mass Transfer* **19**, 471–478.